

# Photovoltaic Cleaning Frequency Optimization Under Different Degradation Rate Patterns

Leonardo Micheli<sup>1</sup>, Marios Theristis<sup>2</sup>, Diego L. Talavera<sup>3</sup>, Florencia Almonacid<sup>1</sup>, Joshua S. Stein<sup>2</sup>, Eduardo F. Fernandez<sup>1</sup>

<sup>1</sup> Center for Advanced Studies in Earth Science, Energy and Environment (CEACTEMA), Photovoltaic Technology Research Group (PVTech-UJA), Las Lagunillas Campus, University of Jaén (UJA), Jaén 23071, Spain.

<sup>2</sup> Sandia National Laboratories, Albuquerque, 87185, NM, USA

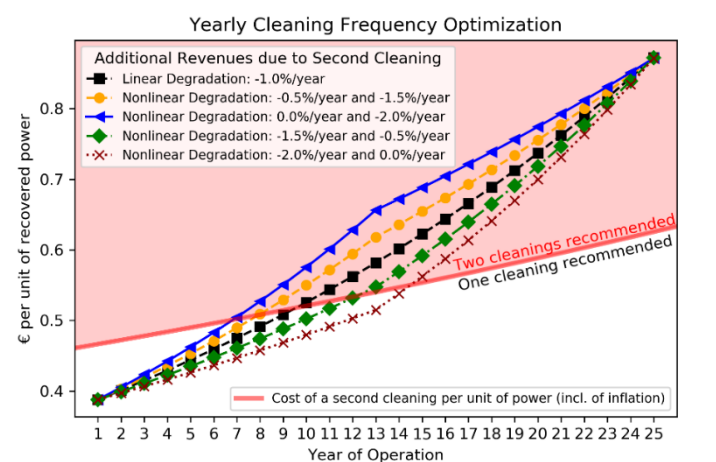
<sup>3</sup> IDEA Research Group, University of Jaén, Campus Lagunillas, 23071, Jaén, Spain

## Abstract

Dust accumulation significantly affects the performance of photovoltaic modules and its impact can be mitigated by various cleaning methods. Optimizing the cleaning frequency is essential to minimize the soiling losses and, at the same time, the costs. However, the effectiveness of cleaning lowers with time because of the reduced energy yield due to degradation. Additionally, economic factors such as the escalation in electricity price and inflation can compound or counterbalance the effect of degradation on the soiling mitigation profits. The present study analyzes the impact of degradation, escalation in electricity price and inflation on the revenues and costs of cleanings and proposes a methodology to maximize the profits of soiling mitigation of any system. The energy performance and soiling losses of a 1 MW system installed in southern Spain were analyzed and integrated with theoretical linear and nonlinear degradation rate patterns. The Levelized Cost of Energy and Net Present Value were used as criteria to identify the optimum cleaning strategies. The results showed that the two metrics convey distinct cleaning recommendations, as they are influenced by different factors. For the given site, despite the degradation effects, the optimum cleaning frequency is found to increase with time of operation.

**Keywords:** Soiling; Cleaning Frequency; Optimization; Photovoltaics; Degradation Rate; Economics.

## Graphical Abstract



The optimum cleaning frequency of a PV system varies with time of operation. The profitability of cleaning is affected by the PV degradation rate pattern and the variability of electricity price and cleaning costs. This work analyzes the separation line that defines the most cost effective cleaning frequency at each year of operation.

## 29 Highlights

- 30 · The optimum cleaning schedule varies depending on time of operation and health state
- 31 · Different cleaning schedules can be recommended based on the LCOE and NPV
- 32 · PV degradation does not affect the LCOE based cleaning decision algorithm
- 33 · Inflation influences the profitability of cleaning schedule over time
- 34 · Nonlinear degradation affects the cleaning frequency and its profitability

## 35 Nomenclature

$C$ [€/kW]	Installation Costs
$CC_s$ [€/kW]	Initial Surface Cleaning Cost
$CC_w$ [€/kW]	Specific Cost of Cleaning
$d$ [%]	Discount Rate
$D_n$ [€/kW/year]	Annual tax depreciation
$E$ [kWh/kW/day]	Daily Energy Yield
$E_s$ [kWh/kW/year]	Soiling ratio-corrected energy yield
$i$	Day of the year
$LCOE$ [€/kWh]	Levelized Cost of Electricity
$n$	Year of operation
$N$ [Years]	PV system lifetime
$n_{c,n}$	Number of yearly cleanings in year $n$
$N_d$ [year]	Depreciation period
$NPV$ [€/kW]	Net present value
$OM_n$ [€/kW/year]	Yearly Operating and Maintenance Costs
$p$ [€/kWh]	Initial price of electricity, taxes included
$P_{DC}$ [kW]	DC capacity of the PV system
$p_{pre-tax}$ [€/kWh]	Initial price of electricity before taxes
$P_{type}$ [kW]	Installed capacity of the PV modules of a specific type
$PV[I(N)]$ [€/kW]	Present value of the inflows
$PV[O(N)]$ [€/kW]	Present value of the outflows
$R_D$ [%/year]	Degradation Rate
$f_D$ [%]	Degradation Factor
$r_{om}$ [%/year]	Annual escalation rate of the O&M costs
$r_p$ [%/year]	Annual escalation rate of the electricity price
$r_s$	Daily Soiling Ratio
$T$ [%]	Income Tax
$VAT$ [%]	Value-added tax
$\eta_{type}$ [%]	Efficiency of the PV modules of a specific type

## 36 1. Introduction

37 Active monitoring of photovoltaic (PV) performance is critical for ensuring the highest energy yield  
38 and profit, as it makes it possible to maximize the efficiency and the revenues of photovoltaic power  
39 plants through improved operation and maintenance (O&M) strategies. The ability to accurately  
40 predict the projected energy yield of such systems by also identifying trend-based performance losses  
41 allows condition-based maintenance strategies, which are important for minimizing O&M costs and,  
42 hence, improving the financial payback of a PV project.

43 Sources of performance loss can be either reversible (i.e., lost energy can be recovered by  
44 maintenance) or irreversible (i.e., lost energy is unable to be recovered unless the component is  
45 completely replaced) [1]. Examples of reversible performance loss include dust deposition (i.e. soiling),  
46 snow, vegetation, fuse failures etc. whereas irreversible performance loss may occur due to several  
47 degradation mechanisms such as discoloration, delamination, hot spots, cracks etc. In order to  
48 account for the performance loss in PV power prediction models, a degradation rate value is usually  
49 considered, which is either taken as an assumption or extracted from a statistical model [2,3]. Such  
50 models, however, have no knowledge of whether the loss is due to reversible or irreversible effects.  
51 Furthermore, routine maintenance due to reversible performance loss, such as cleaning frequency of  
52 PV modules, is commonly executed at a fixed rate per year during the project's lifetime.

53 Field data demonstrated that irreversible performance loss rates may not always be constant (i.e.,  
54 linear) [4–6] due to a number of degradation modes that can occur during the initial and wear-out  
55 phases of a PV system's lifetime. Even when the same lifetime performance loss is assumed under  
56 different linear and nonlinear degradation rate patterns, the economic impact will vary [4,5].  
57 Therefore, due to the different paths of performance loss that could be observed, it is important to  
58 optimize the maintenance strategies on a condition-based manner because the energy recovery and  
59 corresponding financial gains will depend on the system's health-state, inflation etc. In order to  
60 achieve this, algorithms must be developed to respond quickly and intelligently to different  
61 operational issues.

62 Soiling is one of the most common reversible performance losses experienced by PV modules, as it  
63 can generally be removed by natural or artificial cleaning. Rainfall is the most frequent natural cleaning  
64 process [7,8]. Artificial cleanings are performed by O&M operators or robots, and their cost depends  
65 on a number of factors, which vary depending on the geographical location; even within the same  
66 country [9]. If not mitigated, soiling can cause significant economic losses [10,11]. Furthermore, the  
67 impact of soiling is likely to be more severe in future; this is due to the combination of increased  
68 deployment of PV modules in regions characterized by high insolation and soiling and the improved  
69 PV module efficiencies [9]. As such, soiling mitigation strategies must be optimized in order to  
70 maximize the energy output of the system, while minimizing the cleaning expenses.

71 In 2010, Mani and Pillai listed some recommendations for soiling mitigation strategies based on the  
72 climatic zone and the characteristics of the region where PV systems are located [12]. These are useful  
73 guidelines, but the mitigation strategy should always be refined depending on the specific conditions  
74 of each site [13,14]. Several cleaning optimization methods have been proposed in literature to  
75 maximize the profits [15–18]. These are useful methods to determine the optimum cleaning schedule  
76 at given conditions, but they do not consider that the “value” of recovered energy (i.e., difference in  
77 revenue before and after cleaning) changes with time, mainly due to the system's health state and, in  
78 particular, degradation. Indeed, as discussed by Urrejola et al. [19], PV degradation lowers the energy  
79 yield with time. This translates directly into a lower cash inflow and makes cleaning less effective with  
80 the time of operation, considering that the impact of some economic parameters also changes. In

81 particular, the rise of the cleaning costs caused by inflation can compound the impact of degradation,  
82 because cleaning would become more expensive with time.

83 In addition, it should be considered that, in some countries, the electricity price is subject to a daily  
84 market-based competition [20]. This means that the price of electricity sold by the PV system producer  
85 to the grid may vary over time, depending on supply and demand. In these markets, an escalation in  
86 the price of electricity can, at least partially, counterbalance the effects of degradation and rise in  
87 cleaning costs, increasing revenues, and therefore incentivize the cleanings. Taking these factors into  
88 account, along with the influence of discount rate, one could expect that the optimum cleaning  
89 schedule that maximizes the revenues and minimizes the costs would vary with the year of operation.

90 In order to verify this hypothesis, a sensitivity analysis was performed to investigate the impact of  
91 different PV degradation rate patterns on the profitability of cleaning schedules taking into account  
92 the variability of economic parameters and soiling profiles extracted from a 1 MW PV plant in Spain.  
93 A similar analysis was conducted on a PV system in Chile [19] taking into account fixed values for  
94 electricity price and cleaning costs whereas the degradation rate was based on a fixed performance  
95 loss value extracted from a 2-year period. A model to optimize the optimal cleaning schedule also  
96 based on linear degradation and fixed electricity price and cleaning costs was recently presented by  
97 Alvarez et al. [21]. In the present work, these economic parameters are realistically modeled to vary  
98 annually, and the effects of their variation is thoroughly discussed. For the first time, different  
99 degradation rate patterns are considered enabling the cleaning schedule optimization over time using  
100 the levelized cost of electricity (LCOE) and net present value (NPV) metrics as criteria.

101 The paper is structured as follows. The methodologies to analyze the PV performance data, to extract  
102 the soiling profile and to calculate the effects of different cleaning scenarios and degradation rate  
103 patterns are described in 2.1. The economic parameters and equations are detailed in 2.2, whereas  
104 the cleaning optimization process is described in 2.3. The results' section is split into two subsections:  
105 in 3.1, the cleaning frequency is optimized for every year of the PV plant operation considering  
106 different linear degradation rate values and various inflation and electricity price scenarios whereas,  
107 in 3.2, nonlinear degradation rate patterns are introduced and their effects on the profitability of  
108 different cleaning frequencies are discussed.

## 109 2. Methodology

### 110 2.1. PV performance

111 The energy performance and soiling profiles considered in this study were extracted from a real PV  
112 installation, whereas the degradation rate patterns were theoretical and based on previous  
113 investigations [4,5,22]. The methodology used to process the performance timeseries is described in  
114 2.1.1. Subsequently, the methodologies employed, and the assumptions made to calculate the soiling  
115 loss profile and the optimal cleaning schedule are discussed in 2.1.2. Finally, the degradation profiles  
116 modelled in this work are reported in 2.1.3.

#### 117 2.1.1. PV data analysis

118 1-year of hourly data from a 1 MW system installed in the province of Granada, in Southern Spain,  
119 were considered. The system consists of mono-crystalline modules facing South and mounted at a tilt  
120 angle of 30°. The installed DC capacity is 961 kW and no inverter clipping was observed. The energy  
121 yield and soiling profiles were extracted using the same methodology employed by Micheli *et al.* [23],  
122 considering the weather data downloaded from MERRA-2 [24]. The following PV corrections, available  
123 in the *pvlb-python* library [25], were employed to analyze the performance of the site:

124     • The ASHRAE transmission model for the angular correction of incident light [26,27],  
125     • Sandia PV Array Performance Model for the spectral and temperature corrections [28]. All  
126     coefficients were sourced from the Sandia PV Module Database.

127     The absolute and relative air mass [29,30] were defined from the apparent zenith, calculated with the  
128     solar position algorithm [31], and the MERRA-2 site air pressure.

### 129     2.1.2. Soiling extraction

130     Soiling is commonly quantified through two metrics: the soiling ratio and the soiling rate. The soiling  
131     ratio expresses the ratio of the output of the soiled PV system to the output of the PV system without  
132     soiling [32]. It has a value of 1 in clean conditions and decreases as soiling accumulates. The soiling  
133     losses can be expressed as  $(1 - \text{soiling ratio})$ . On the other hand, the soiling rate quantifies the rate at  
134     which soiling deposits on the PV modules and is calculated as the daily derate in soiling ratio (i.e. slope  
135     of the soiling ratio profile), expressed in %/day and reported in negative values [33]. A soiling rate of  
136     0%/day occurs when there is no soiling being deposited, and its value decreases as the soiling  
137     deposition rate increases.

138     The daily soiling ratio values were extracted from the aforementioned performance data, considering  
139     only the hours near noon on high-irradiance days [32]. To ensure relatively clear-sky conditions, only  
140     data conditions when plane-of-array irradiance was  $> 700 \text{ W/m}^2$  was used. This threshold is higher  
141     than that used previously [34,35], but it minimizes the noise in the soiling ratio estimation.

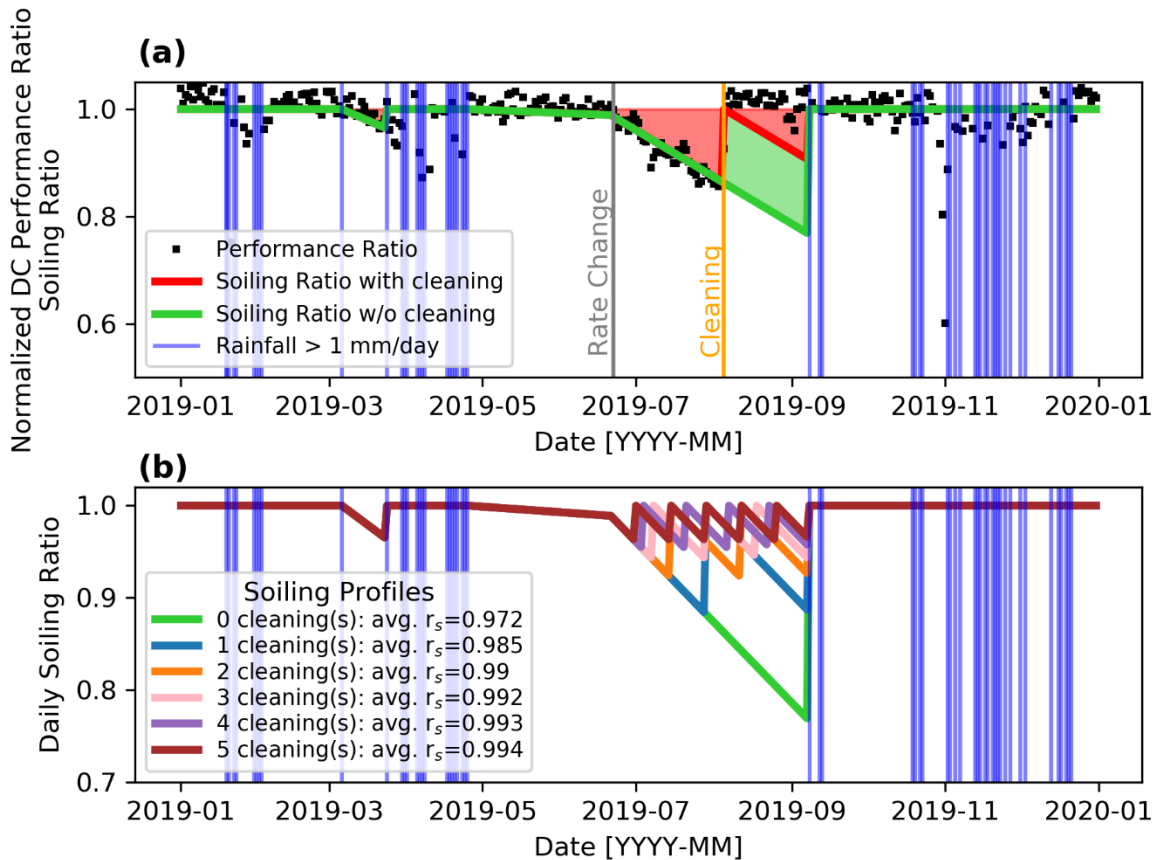
142     The soiling ratio profile is shown in Figure 1a. The investigated site is characterized by seasonal soiling,  
143     with a long summer period of no rain exhibiting a peak power loss of 23% at the beginning of  
144     September. This results in a soiling rate of -0.28%/day occurring from mid-June to the end of the  
145     summer. A change in soiling rate occurred on June 22<sup>nd</sup> due to a dust-laden wind [23,36].

146     The aim of this work was to analyze the optimum number of cleanings (i.e. cleaning frequency) that  
147     would maximize the profits from soiling mitigation. To do that, it was necessary to understand the  
148     extent of the soiling losses if no mitigation actions had been in place (worst-case scenario of no  
149     cleaning) and therefore to extract the natural soiling profile of the site. For this reason, the effect of  
150     the artificial cleaning event performed by the O&M team on August 5<sup>th</sup> was removed. As such, the  
151     positive shift in the soiling ratio profile on August 5<sup>th</sup> was eliminated by propagating the same soiling  
152     rate (i.e., -0.28%/day) until the following rain event in September (see green line in Fig. 1a for natural  
153     soiling profile). Similarly, artificial cleanings are modelled in a way to produce a sudden positive shift  
154     in the soiling ratio profile, restoring its value to 1, but without a change in soiling rate (i.e., soiling rate  
155     before cleaning is equal to soiling rate after cleaning). This decision is already employed in other  
156     cleaning optimization studies [15,37] and is based on the assumption that cleaning washes off  
157     deposited dust from the modules and does not have any effect on the external atmospheric conditions  
158     that cause soiling deposition (such as suspended particle concentration, wind speed, relative humidity  
159     [38,39]). Consensus has not yet been reached within the community regarding “grace periods” (i.e., a  
160     fixed number of days following a cleaning event in which soiling does not deposit on the PV modules)  
161     [15,33,40]. Therefore, soiling was assumed to accumulate on the PV surfaces immediately after a  
162     cleaning event, without any “grace period” [37].

163     In a “no cleaning performed” assumption (green line in Fig. 1a), it is estimated that the AC energy yield  
164     of the system would have been 1691 kWh/kW, with an average soiling loss of 2.8%. This represents  
165     the worst-case scenario, in which no mitigation is put in place to address soiling. The soiling profile in  
166     this site can be considered as representative for southern Europe and a number of Southwestern US  
167     States, including California, due to the combination of low and infrequent precipitation and elevated  
168     levels of suspended dust, which are commonly observed during the summer months. Similar yearly  
169     losses, in the order of 3 to 4% were reported for a number of studies worldwide [41–43]. Therefore,

170 the results extracted from this study could be associated with installations exposed under similar  
 171 climatic locations elsewhere.

172 Ideally, if soiling was completely removed (i.e. soiling loss of 0%), the yield would have been  
 173 1748 kWh/kW. It should be noted that the energy yield variation is larger than the average soiling loss  
 174 because the highest dust deposition occurs in summer. This yield represents the best-case scenario  
 175 and is used as a baseline to quantify the benefits of different cleaning frequencies. Six potential  
 176 cleaning schedules were considered in this study and their effects on the soiling profile are shown in  
 177 Fig. 1b. The considered schedules include cleaning frequencies ranging from 0 to 5 times per year,  
 178 which are assumed to be performed on the dates that maximize the soiling ratio (i.e. minimize the  
 179 energy losses). Similar to the procedure described by Micheli *et al.* [40], for each frequency, a soiling  
 180 profile is modelled for each possible combination of cleaning dates. The dates that return the highest  
 181 average soiling ratio (i.e. the minimum annual losses) are the optimal cleaning dates for each given  
 182 cleaning frequency scenario. These six optimized soiling profiles are analyzed in the rest of the paper,  
 183 introducing the economic metrics and parameters described in Section 2.2, in order to identify the  
 184 most cost competitive cleaning frequency (i.e. the one that maximizes the difference between  
 185 revenues and cleaning costs). For the purposes of this study, the soiling profile was assumed to repeat  
 186 every year of operation and no change in soiling rate was considered after each cleaning [18,36].



187  
 188 Fig. 1. (a) Soiling and performance profiles of a 1 MW power plant located in Granada, Spain. The black dots represent the  
 189 DC performance ratio normalized to the median value and the red line shows the extracted soiling profile including the August  
 190 5th cleaning event (marked with a yellow vertical line); the modeled soiling profile without considering any cleaning is also  
 191 displayed with green color. The blue vertical lines are the rainfall events whereas the change in soiling deposition rate is  
 192 marked with a grey vertical line. (b) Soiling profiles for optimized cleaning schedules with different frequencies ranging from  
 193 0 to 5 times per year. The average daily soiling ratios are also shown for each scenario.

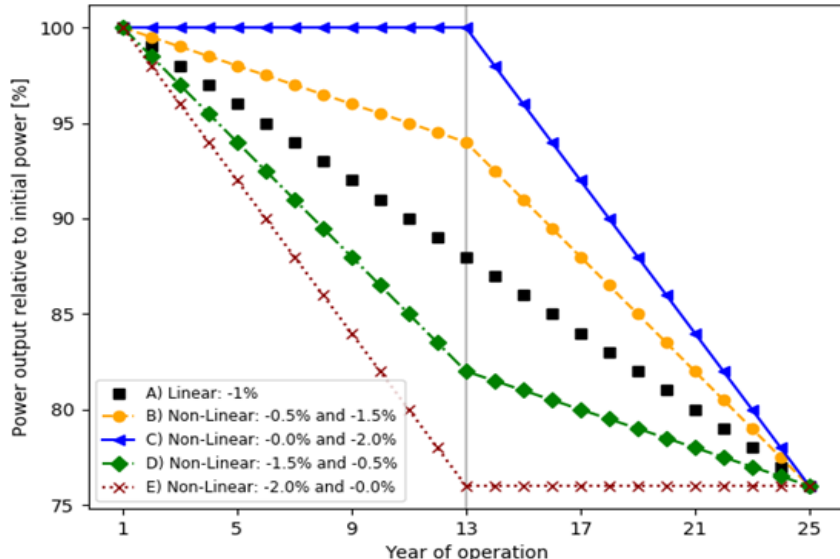
194 2.1.3. Performance degradation profiles

195 The aforementioned energy yield did not include the effect of degradation, which was modelled from  
 196 synthetic data. Five different performance loss patterns were considered as illustrated in Fig. 2. These  
 197 include:

- 198 A. Linear degradation of -1.0%/year,
- 199 B. Nonlinear: -0.5%/year initially followed by -1.5%/year,
- 200 C. Nonlinear: 0%/year initially followed by -2.0%/year,
- 201 D. Nonlinear: -1.5%/year initially followed by -0.5%/year,
- 202 E. Nonlinear: -2.0%/year initially followed by 0%/year.

203 All nonlinear degradation patterns assume that the rate changes in year 13 (out of 25 years of  
 204 operation). Similar to [4,5,22], the theoretical linear and nonlinear patterns were selected in a way to  
 205 reflect the same power loss at the end of the system's lifetime (i.e., 24% loss of power in year 25).  
 206 Although the patterns are normalized to cover a 25-year lifetime, they could represent early life  
 207 degradation modes such as light and elevated temperature induced degradation (LeTID) [44] observed  
 208 in Passivated Emitter and Rear Contact (i.e. PERC) PV modules, light induced degradation [45] in  
 209 crystalline silicon PV modules, and Staebler-Wronski [46] effects in amorphous silicon. Such types of  
 210 degradation occur at various time scales from a number of hours to years [4,5,22]. Furthermore,  
 211 depending on the degradation-regeneration cycle of LeTID, PERC modules could potentially exhibit  
 212 minimal to even positive "degradation" rate in the field [47].

213 For the purposes of this work, the various strings and inverters of the PV system are assumed to  
 214 degrade and soil at the same rate. Further studies will be conducted in future, as new data become  
 215 available, on the non-uniformity of soiling and degradation within a given site.



216  
 217 Fig. 2. Theoretical degradation rate profiles considered in this study.

218 2.2. Economic metrics and parameters

219 The cleaning schedule optimization against different degradation scenarios was assessed using the  
 220 LCOE and NPV as criteria. Depending on the metric, the optimization was realized by selecting the  
 221 cleaning frequency that either minimized the LCOE or maximized the NPV (see 2.3). The values of the  
 222 economic metrics were calculated for each of the soiling profiles (Fig. 1b) and degradation rate  
 223 scenarios (Fig. 2), taking into account the cost of the corresponding cleaning and the revenues granted

224 by the corresponding energy yield. The methodologies used to calculate each of the economic metrics  
 225 are independently discussed in the following subsections: 2.2.1 (LCOE) and 2.2.2 (NPV).

## 226 2.2.1. Levelized Cost of Electricity

227 The LCOE quantifies the unitary cost of each kWh of electricity generated, considering its entire  
 228 lifecycle and is defined as [48]:

$$LCOE = \frac{C + \sum_{n=1}^N \frac{(OM_n + n_{c,n} \cdot CC_w) \cdot (1 - T) \cdot (1 + r_{om})^n}{(1 + d)^n} - \sum_{n=1}^{N_d} \frac{D_n}{(1 + d)^n} \cdot T}{\sum_{n=1}^N E_s(n_{c,n}) \cdot f_D(n) / (1 + d)^n} \quad (1)$$

229 where C are the installation costs, OM<sub>n</sub> the yearly O&M costs, n<sub>c,n</sub> the number of yearly cleanings (i.e.  
 230 cleaning frequency on the year n), CC<sub>w</sub> the initial Specific Cost of Cleaning (in €/W), T the income tax,  
 231 r<sub>om</sub> the annual escalation rate of O&M costs, d the discount rate, E<sub>s</sub> the soiling ratio–corrected energy  
 232 yield, f<sub>D</sub>(n) a factor taking into account the effect of degradation, D<sub>n</sub> is the annual tax depreciation for  
 233 the PV power plant. The values of the parameters used in (1) are reported in Table 1. In this analysis,  
 234 the annual escalation rate of the O&M costs was set to be equal to the inflation rate. Tax depreciation  
 235 allows recovering part of the investment cost through reduced taxes and has been assumed to be  
 236 linear and constant over a given period of time (N<sub>d</sub>) [49]. It is acknowledged that the method used to  
 237 model tax depreciation (e.g. straight line or declining balance) can affect the analysis.

238 The soiling ratio–corrected energy yield, E<sub>s</sub>, used in (1), is calculated as:

$$E_s(n_{c,n}) = \sum_{i=1}^{365} r_{s,nc}(i) \cdot E(i) \quad (2)$$

239 with r<sub>s,nc</sub> being the soiling ratio for a n<sub>c,n</sub> number of yearly cleanings as shown in Fig. 1b and E is the  
 240 daily energy yield profile in no soiling conditions. E<sub>s</sub> has a value of 1748 kWh/kW/year in conditions of  
 241 no soiling and lowers to a minimum of 1691 kWh/kW/year when soiling and no cleaning are  
 242 considered. In this work, the degradation rate is assumed to affect the annual soiling ratio – corrected  
 243 energy yield, rather than the daily performance profiles and for this reason is present in (1) through  
 244 the factor f<sub>D</sub> and not in (2). Assuming linear degradation R<sub>D</sub>, the factor f<sub>D</sub> can be calculated as:

$$f_D(n) = (1 + R_D)^n \quad (3)$$

245 On the other hand, if degradation rate is indeed nonlinear, the equations can be rewritten to take into  
 246 account the two different rates, R<sub>D1</sub> and R<sub>D2</sub> (as shown in Fig. 2):

$$f_D(n) = (1 + R_{D1})^{n_1} \cdot (1 + R_{D2})^{n_2} \quad (4)$$

247 where n<sub>1</sub> and n<sub>2</sub> are the number of years in which R<sub>D1</sub> and R<sub>D2</sub> occurred, respectively, and follow these  
 248 rules: n<sub>1</sub>+n<sub>2</sub>=n, n<sub>2</sub>=0 if n < N/2, n<sub>1</sub>=N/2 if n ≥ N/2.

249 The term CC<sub>w</sub> used in (1) is referred to as “initial” because the cleaning cost varies with time according  
 250 to the escalation rate of the O&M costs (r<sub>om</sub>). In particular, it can be derived from the Surface Cleaning  
 251 Cost (CC<sub>s</sub>) following the methodology detailed in [9,23]:

$$CC_w \left[ \frac{\text{€}}{\text{kW}} \right] = \sum_{type} \frac{\frac{CC_s}{\text{kW}} \cdot P_{type}}{\frac{\eta_{type} \cdot 1 \frac{\text{kW}}{\text{m}^2}}{P_{DC}}} \quad (5)$$

252 where P<sub>DC</sub> is the DC capacity (961 kW), and η<sub>type</sub> and P<sub>type</sub> is the nameplate efficiency and power of the  
 253 installed PV modules.

## 254 2.2.2. Net Present Value

255 The second metric used in this work to estimate the economics of various cleaning frequencies is the  
 256 Net Present Value (NPV). The NPV compares revenues and costs over the lifetime of the projects. An  
 257 investment is considered profitable when  $NPV > 0$ . In this work, the following equation has been  
 258 adopted:

$$259 \quad NPV = -C + PV[I(N)] - PV[O(N)] \quad (6)$$

260 where the present value of inflows  $PV[I(N)]$  and outflows  $PV[O(N)]$  over a project's lifetime are defined  
 as:

$$261 \quad PV[I(N)] = \sum_{n=1}^N \frac{p \cdot E_s(n_{c,n}) \cdot (1 - T) \cdot f_D(n) \cdot (1 + r_p)^n}{(1 + d)^n} + \sum_{n=1}^{n_d} \frac{D_n}{(1 + d)^n} \cdot T \quad (7)$$

$$262 \quad PV[O(N)] = \sum_{n=1}^N \frac{(OM_n + n_{c,n} \cdot CC_w) \cdot (1 - T) \cdot (1 + r_{om})^n}{(1 + d)^n} \quad (8)$$

263 where  $p$  is the price of electricity and  $r_p$  the average annual rate of increase in the price. The price of  
 264 electricity is calculated as:

$$265 \quad p = p_{pre-tax} \cdot (1 + VAT) \quad (9)$$

266 where  $p_{pre-tax}$  is the initial price of electricity before taxes, and VAT is the value-added tax (21%). The  
 267 average yearly pre-tax price of electricity is affected by several factors and can vary with time and  
 268 location depending on the available supply and demand. Similar to the cleaning cost,  $p$  is considered  
 269 as an *initial* electricity price, because its value varies with the year of operation.

270 The majority of existing PV plants in Spain, where this investigation is conducted, sell their energy  
 271 directly to the electricity market. This direct sale of produced electricity has become extremely popular  
 272 and profitable - for the past three years due to the combination of consistently high electricity prices  
 273 and falling costs of PV installations. Spanish banks have long experience in financing photovoltaic  
 274 projects and have been financing only those installations that sell their electricity on the market [50].  
 275 For these reasons, a varying electricity price has been taken into account as a primary scenario. In  
 276 particular, the value of  $r_p$  was set equal to the average annual increase in electricity price in Spain for  
 277 the last 10 years [51,52]. Despite that, power purchase agreements (PPAs) are a common practice in  
 278 many countries and PPAs are effective in some new PV projects in Europe [53]. This scenario,  
 represented by an  $r_p$  of 0%/year, is also discussed in the paper.

279 *Table 1. Economic parameters used in this study and sourced from the literature for utility-scale PV systems in Spain. The*  
 280 *asterisk marks that the value has been converted from U.S. dollars, considering a 0.92 \$/€ conversion factor.*

Parameter	Symbol	Value	Units	References
Years of operation	N	25	years	
O&M costs, cleaning excluded	OM <sub>n</sub>	15	€/kW/year	[48]*
Installation Costs	C	700	€/kW	[54]
Initial Surface Cleaning Cost	CC <sub>s</sub>	0.09	€/m <sup>2</sup> /cleaning	[9]
Specific Cost of Cleaning	CC <sub>w</sub>	0.62	€/kW/cleaning	calculated from (5)

Discount Rate	d	6.4	%/year	[48]
Annual escalation rate of the operation and maintenance cost	$r_{om}$	1.23	%/year	[55]
Income Tax	T	25	%	[48]
Depreciation period	$N_d$	20	years	[49]
Average annual rate of increase in the electricity price	$r_p$	4.48	%/year	[51,52]
Value added tax	VAT	21	%	[49]
Initial pre-tax price of electricity	$p_{pre-tax}$	0.04778	€/kWh	[51,52]

### 2.3. Yearly Cleaning Frequency Optimization

The cleaning frequencies that minimize the LCOE and maximize the NPV were calculated in this work for each year of the system's lifetime. Compared to previous studies [19,21], where fixed numbers of cleanings throughout the lifetime of the system were assumed, in this case, the optimum cleaning frequency was varied with time due to performance degradation, electricity price, and O&M costs. The cleaning frequency that minimized the LCOE in each  $n$ -year of operation was found using the following formulation:

$$\min \left( \frac{(OM_n + n_{c,n} \cdot CC_w) \cdot (1 - T) \cdot (1 - r_{om})^n}{E_s(n_{c,n}) \cdot f_D(n)} \right) \quad (10)$$

with  $0 \leq n_{c,n} \leq 5$  and the values described in Table 1. Similarly, the cleaning frequency that maximized the NPV in each  $n$ -year of operation was found using the following formulation:

$$\max \left( \frac{p \cdot E_s(n_{c,n}) \cdot (1 - T) \cdot f_D(n) \cdot (1 + r_p)^n}{(1 + d)^n} - \frac{(OM_n + n_{c,n} \cdot CC_w) \cdot (1 - T) \cdot (1 + r_{om})^n}{(1 + d)^n} \right) \quad (11)$$

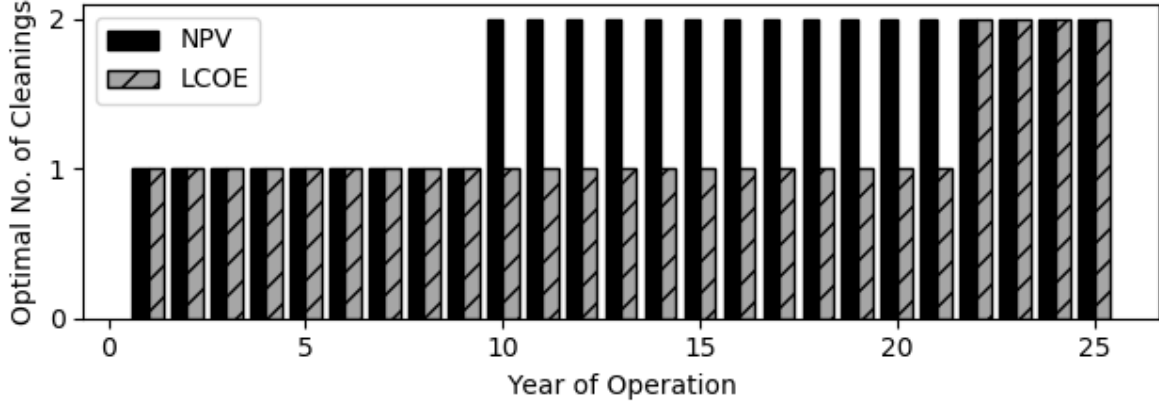
The cleaning frequencies returning the minimum LCOE and maximum NPV were found by comparing the results of each potential cleaning scenario for every year of operation. Therefore, for each of the 25 years of operation, six values were calculated and compared to solve (10) and six additional values were calculated and compared to solve (11). It should be highlighted that the cleaning frequency ( $n_{c,n}$ ) does not affect the degradation rate (quantified in  $f_D$ , see (3) and (4)), but it can only modify the soiling profiles used to calculate  $E_s$  (see (2)). Furthermore, performance degradation affects the profitability of each cleaning, because it reduces the amount of energy that each cleaning can recover. Therefore, one can expect lower profits after each cleaning as the PV system degrades. However, while the energy recovery lowers with time, other parameters in (10) and (11) can influence the economic effect of degradation on the cleaning frequency; these are being investigated in Section 3.

## 3. Results and Discussion

### 3.1. Yearly Schedule Optimization

In this section, the cleaning frequency that minimizes the LCOE and maximizes the NPV for each year of the system's lifetime is discussed assuming a linear degradation scenario. Compared to the previous studies [19,21,23], where fixed numbers of cleanings throughout the system lifetime were assumed,

303 in this case, the optimum cleaning frequency is allowed to vary with time due to performance  
 304 degradation, electricity price, and O&M costs. The results of this analysis for the two economic metrics  
 305 considered in this study are shown in Fig. 3. As expected, the optimum cleaning frequency indeed  
 306 changes with time. Under the given conditions, both metrics are found to favor more frequent  
 307 cleanings towards the end of the life of the system.



308  
 309 *Fig. 3. Optimum cleaning frequency as a function of LCOE and NPV, in presence of a linear degradation rate of -1%/year*  
 310 (*Scenario A*).

311 To maximize NPV, it is recommended to switch to two cleanings/year in year 10, while to minimize  
 312 LCOE, the switch is recommended in year 22. The different results are due to the different structures  
 313 of the metrics. If (1) is solved for the cleaning cost, it is found that, in order to minimize the LCOE, the  
 314 switch from a schedule of  $n_{c,n}$  cleanings/year to  $n_{c,n}+1$  cleanings/year occurs in year  $n$  in which the  
 315 following criterion is met:

$$< \frac{(1 + r_{om})^n \cdot CC_W \left[ \frac{\epsilon}{kW} \right] \left( \frac{E_s(n_{c,n} + 1)}{E_s(n_{c,n})} - 1 \right) \cdot \left( (1 + d)^n \cdot \frac{C}{N} + OM_{t,n} \cdot (1 + r_{om})^n \cdot (1 - T) - D_n \cdot T \cdot [n \leq Nd] \right)}{(1 - T)} \quad (12)$$

316 where  $E_s(n_{c,n} + 1)$  and  $E_s(n_{c,n})$  are the corresponding energy yields for  $n_{c,n}+1$  and  $n_{c,n}$  cleanings/year.  
 317 First, the equation shows that the LCOE-based cleaning decision is independent of the degradation  
 318 rate. This is due to the fact that the degradation has the same effect on the energy yields of the two  
 319 cleaning approaches. This finding should not lead to the misunderstanding that the degradation has  
 320 no impact on the LCOE. Simply, if the LCOE is used as an economic metric, the yearly cleaning schedule  
 321 would not change because of the degradation pattern. Second, for the effect of discounting, the cost  
 322 of cleanings in the calculation of the LCOE becomes less significant year-after-year compared to the  
 323 installation cost, which is the only non-discounted parameter in (1). This becomes even more  
 324 important if the annual tax depreciation is only valid for a number of years  $N_d < N$ . For this reason,  
 325 cleanings toward the end of the PV system life have a lower economic impact on the LCOE and might  
 326 contribute to reducing its overall value.

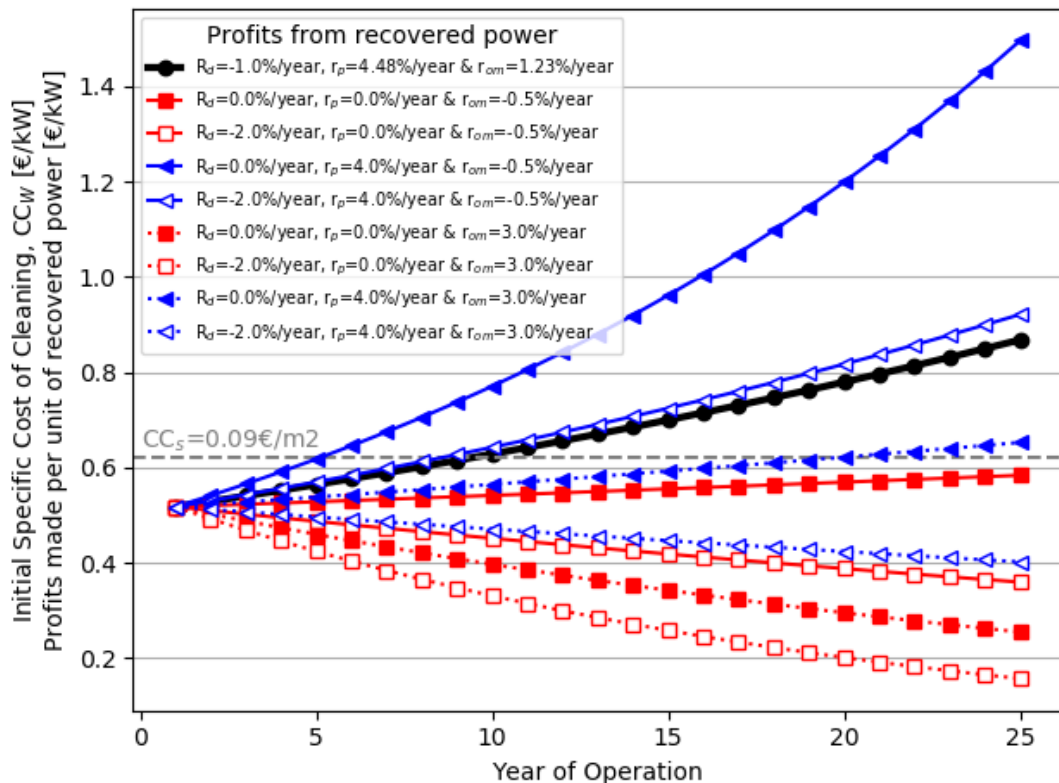
327 On the other hand, when NPV is considered, switching from an  $n_{c,n}$  to an  $n_{c,n}+1$  cleaning schedule  
 328 occurs when the cost of cleaning becomes lower than the profits made per unit of power recovered:

$$(1 + r_{om})^n \cdot CC_W \left[ \frac{\epsilon}{kW} \right] < p \cdot (E_s(n_{c,n} + 1) - E_s(n_{c,n})) \cdot (1 + R_D)^n \cdot (1 + r_p)^n \quad (13)$$

329 As shown in the equation, the discount rate and the income taxes do not affect the cleaning decision  
 330 when NPV is used as the criterion. Also, the installation, fixed O&M costs and depreciation mechanism

331 do not impact the cleaning decision, because they would not be affected by the different energy yields  
 332 and would have the same impact under any cleaning scenarios.

333 The optimum yearly cleaning frequency varies depending on the input parameters. The sensitivity  
 334 analysis taking into account the escalation rate of O&M costs and electricity prices for different  
 335 degradation rates (and patterns) is shown in Fig. 4. As can be seen, the switch in cleaning frequency  
 336 occurs when the value of recovered energy meets the cost of cleaning. According to (13), two  
 337 cleanings/year are more profitable when the value of the recovered energy  $\geq CC_w \cdot (1 + r_{om})^n$ ,  
 338 otherwise one cleaning should be preferred. It should be noted that, under some conditions (e.g.  $r_p =$   
 339 0.0%/year), no switch occurs, while in other cases, more than one switch might be recommended.



340  
 341 *Fig. 4. Sensitivity analysis of NPV taking into account changes in electricity price and O&M costs and in recovered energy*  
 342 *under different values of degradation rate. An additional cleaning is recommended when the profits are higher than the initial*  
 343 *cost of cleanings (grey dashed line). The  $r_p = 0\%/\text{year}$  (i.e. no changes in electricity price) condition is representative for sites*  
 344 *with a fixed PPA in place. In this graph, the NPV values are calculated by moving the term  $(1+r_{om})^n$  from the left-hand side to*  
 345 *the denominator of the right-hand side of (13).*

346 As can be seen in Fig. 4, the slope of the curve increases while (i) the degradation rate decreases, (ii)  
 347 the escalation rate of the O&M costs decreases or (iii) the escalation rate of the electricity price  
 348 increases. The initial price of electricity would not affect the slope but would only change the  
 349 intercept. It is important to highlight, that the slopes can be either positive or negative. A positive  
 350 slope occurs when cleanings become more profitable with time, as long as:

$$|R_d| < 1 - \frac{1 + r_{om}}{1 + r_p} \quad (14)$$

351 These findings confirm that, even if the amount of energy recovered by cleaning decreases because  
 352 of degradation, the inflation and the variation in the cleaning costs can make it possible to profitably  
 353 increase cleaning frequency over time.

354 For the PV site investigated in this work, a cleaning schedule with a variable number of cleanings/year  
355 leads to an increment in NPV < 0.1% compared to the case in which the modules are always cleaned  
356 twice a year. The benefits of this approach should be evaluated on a case-by-case basis, since the  
357 magnitude of this variation changes depending on the severity of degradation rate and values of  
358 discount rate.

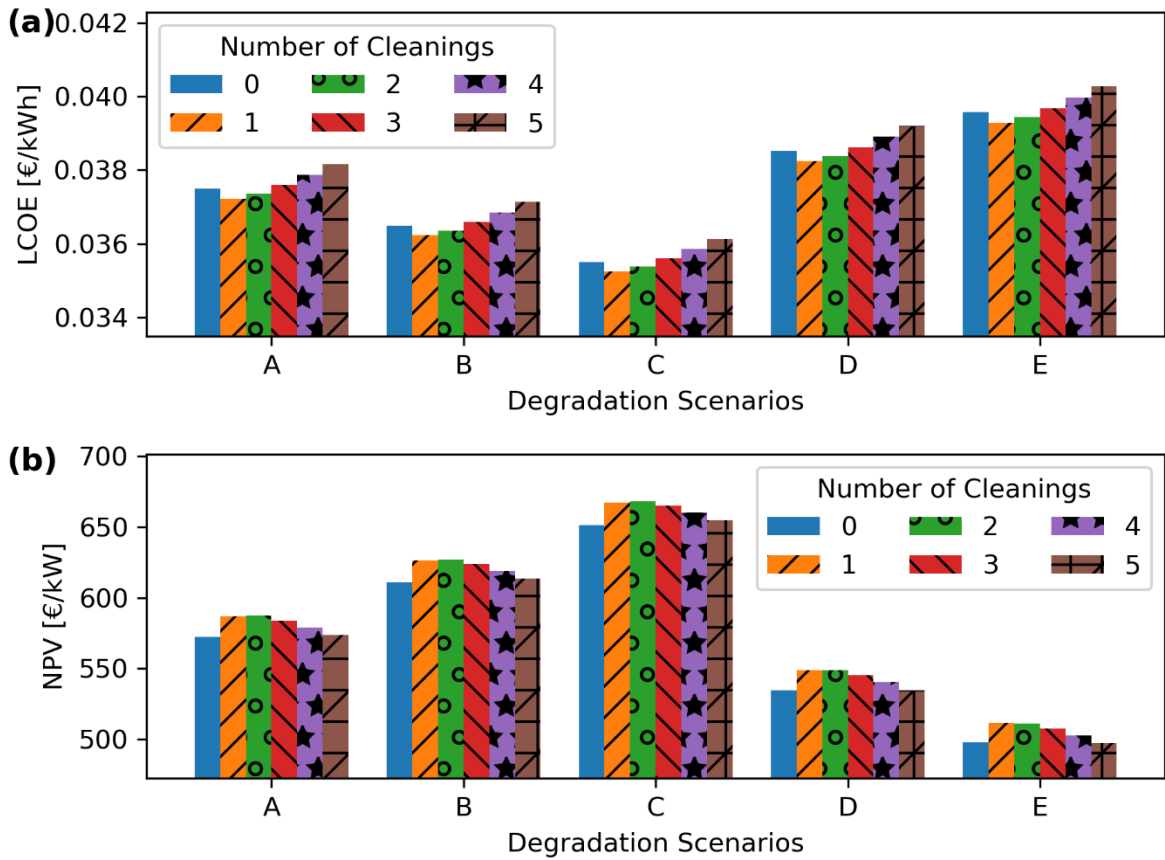
359 Overall, the LCOE and NPV evaluate differently the costs and benefits of the various cleaning  
360 schedules, because the parameters that influence the decision of whether to clean or not are different  
361 (see (12) and (13)). It is interesting to note that the cleaning schedule that maximizes the profits is not  
362 necessarily the one minimizing the cost of electricity and vice versa. At the given soiling conditions, an  
363 LCOE-optimized cleaning schedule would cause a loss in profits of 0.1% compared to an NPV-optimized  
364 cleaning. This loss becomes more substantial as soiling increases; e.g. if the soiling rates were  
365 multiplied by a factor of 1.5x and 3x, the difference in profits would become 0.4% and 0.7%  
366 respectively. In addition, this difference would become more significant for locations with higher  
367 electricity prices. Indeed, higher electricity prices would incentivize more frequent cleanings, while  
368 the LCOE recommendation would not change, since LCOE is not sensitive to electricity price.

### 369 **3.2. Impact of Non-Linear vs. Linear Degradation Rates**

370 The influence of linear degradation rate on the profitability of soiling mitigation was discussed in 3.1.  
371 However, nonlinear degradation rates can have a strong impact on the LCOE and, hence, on the  
372 profitability of a PV project [4,5]. The most profitable cleaning schedule changes depending on the  
373 degradation rate because, given the same soiling ratio, the amount of recovered energy per cleaning  
374 lowers. In this section, the analysis is repeated by taking into account the nonlinear degradation rate  
375 scenarios exhibited in Fig. 2. Initially, a fixed number of cleanings/year are considered for the lifetime  
376 of the system, whereas, in the second part of the section, the cleaning frequency is optimized every  
377 year.

378 Fig. 5 illustrates the impact of the different degradation rate patterns on the LCOE and NPV as a  
379 function of cleaning frequency. The two optimum cleaning strategies include the one with the lowest  
380 cost of electricity for all the degradation rate scenarios and the one returning the highest profits (i.e.  
381 maximum NPV).

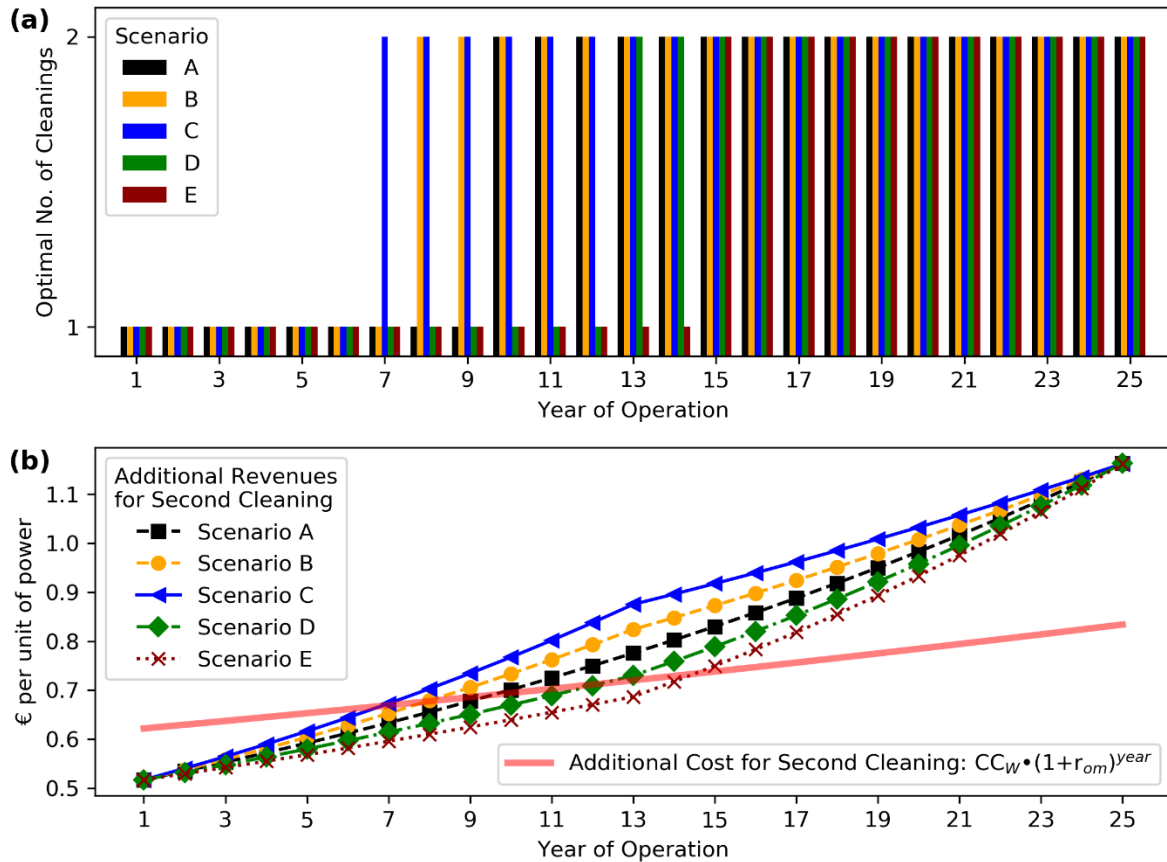
382 Transitioning from a no-cleaning to a single annual cleaning approach leads to a decrease of 0.7% in  
383 LCOE; independently of the degradation rate pattern. When NPV is used as a criterion, the twice a  
384 year-cleaning scenario is the most profitable cleaning schedule for all the degradation scenarios but  
385 the scenario E, which favors a one-cleaning approach. The differences between the one-cleaning and  
386 two-cleaning approaches are limited in all the degradation scenarios. Overall, the optimum cleaning  
387 frequency leads to profit raises of up to 2.7% in the case of NPV, when compared to the no-cleaning  
388 approach (i.e. no soiling mitigation in place).



389  
390 *Fig. 5. a) LCOE and b) NPV values depending on the cleaning frequency for various degradation rate scenarios. The optimum*  
391 *cleaning schedule is the one that minimizes the LCOE and/or maximizes the NPV.*

392 As shown in the previous section, the number of annual cleanings can be optimized every year. In this  
393 analysis, the LCOE metric is neglected since (12) and Fig. 5 demonstrated that an LCOE-based cleaning  
394 decision is not affected by the degradation rate value and/or pattern.

395 The cleaning frequencies were calculated and exhibited in Fig. 6 for the various degradation scenarios  
396 in order to optimize the NPV. As expected, systems with the best performances (i.e. lower initial  
397 degradation rates) require more frequent cleaning for longer periods, because cleaning tends to be  
398 more profitable. These results are explained by Fig. 6b, where the evolution of the cleaning cost,  
399 obtained as  $CC_w \cdot (1 + r_{om})^n$ , is compared to the revenue obtained by moving from a one-cleaning  
400 to a two-cleaning scenario (right-hand side of (13)), which is affected by the degradation rate and by  
401 the annual increase in electricity price. Overall, higher degradation rates lower the slopes of revenue  
402 per cleaning. The switch in cleaning frequency occurs when the cost of cleaning line intercepts the  
403 revenue per cleaning. The high initial degradation modelled in Scenario E keeps the revenue per  
404 cleaning lower than the cost of cleaning for longer time, justifying a one-cleaning approach until year  
405 14 of operation. On the other hand, conditions for a profitable additional cleaning are reached faster  
406 in scenario C, because of the initial lack of degradation.

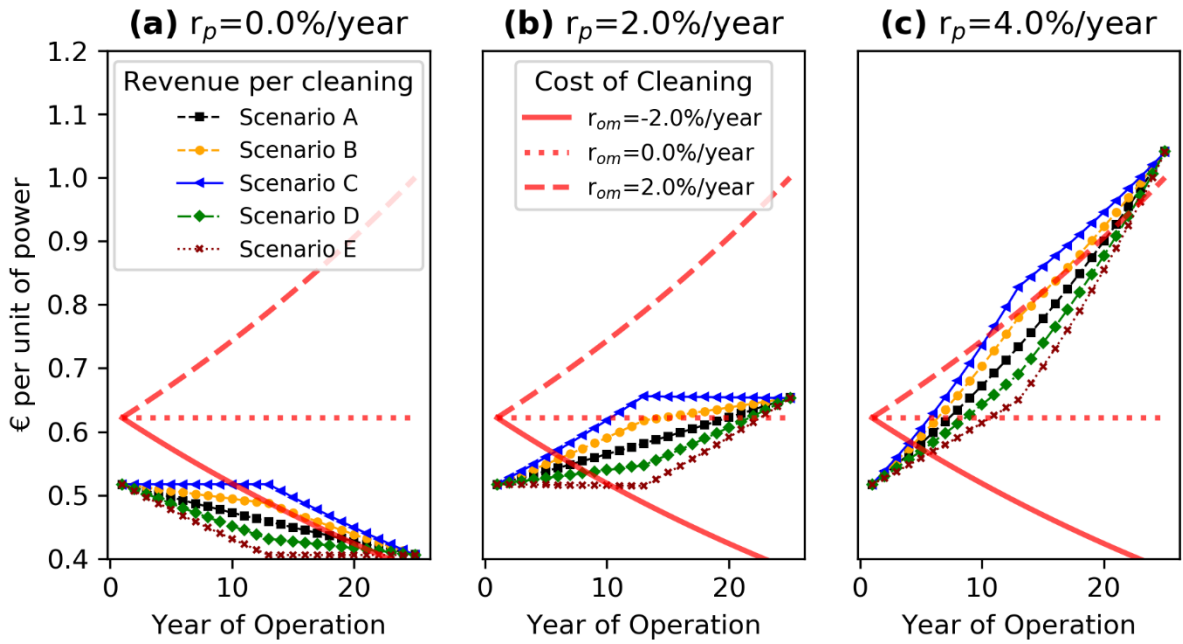


407  
408 *Fig. 6. a) Cleaning frequencies that maximize NPV for different degradation scenarios and b) annual cost of cleaning per unit*  
409 *of power and the trends of revenues per cleaning depending on the degradation rate scenario. An additional cleaning is*  
410 *profitable when the revenue per cleaning is higher than the cost of cleaning.*

411 The slopes of revenue per cleaning lines are positive as long as the degradation rate is lower than the  
412 annual increase in electricity price, which is always true in the investigated case because of the high  
413 electricity price escalation rate (4.48%/year). Each subplot in Fig. 7 shows the additional revenues and  
414 costs of a second cleaning compared to a single cleaning scenario for the investigated site, and  
415 demonstrates how the trends would change for a different value of  $r_p$ . The red lines represent the  
416 cleaning cost escalation rate, ranging from +2%/year (dashed line) to -2%/year (continuous line). The  
417 latter scenario was considered because, given the expected increasing impact of soiling in future [9],  
418 the development and wide-scale deployment of novel cleaning technologies could actually lower the  
419 soiling mitigation costs.

420 The revenue per cleaning lines are flat when  $r_p = R_D$ . As expected, the slopes become negative when  
421 degradation rate becomes greater than the escalation rate in electricity price. This is the case for PV  
422 sites under a power purchase agreement with a fixed price (i.e.  $r_p = 0\%/\text{year}$ , Fig. 7a). In these  
423 conditions, the profits made by cleaning the modules lowers with time. A once/year cleaning scenario  
424 would be recommended, unless the cost of cleaning lowered by 2.0%/year. In this case, Scenario C  
425 would be the fastest in switching to a twice/year cleaning approach.

426 The theoretical examples demonstrated in Fig. 7 return either a fixed number of cleaning frequency  
427 or a switch from one to two annual cleanings. In reality, a switch from twice a year cleaning frequency  
428 to once a year might occur when the increase in cleaning cost is higher than the combined effect of  
429 degradation rate and electricity price inflation.



430  
431 Fig. 7. Additional revenue per cleaning due to recovered energy (lines with markers) and additional cost of a second cleaning  
432 (red lines) for different degradation and inflation ( $r_{om}$ ) scenarios. Each plot takes into account a different escalation rate of  
433 electricity price,  $r_p$ . Plot (a) is representative for sites with a fixed PPA in place ( $r_p = 0.0\%/\text{year}$ ).

## 434 4. Conclusions

435 This study investigated the impact of degradation rate patterns on soiling mitigation strategies taking  
436 into account various economic metrics and parameters. In order to reduce the LCOE or increase the  
437 NPV, the cleaning frequency can vary annually, since the cost of cleaning and value of recovered  
438 energy may also change with time.

439 First, it is found that the degradation rate or pattern does not affect the cleaning frequency decision,  
440 when optimized based on the LCOE. While different degradation scenarios do have an impact on the  
441 absolute LCOE values, the cleaning strategy that minimizes the LCOE is independent of degradation.  
442 On the other hand, the cleaning optimization algorithm based on the NPV neglects the discount rate,  
443 income taxes and depreciation. This leads to different results for the two approaches and means that  
444 a cleaning schedule that maximizes the profits could affect the cost of electricity and vice versa.  
445 Because of the relatively low soiling rates at the investigated site, the NPV- and LCOE-based  
446 approaches showed limited differences, which are expected to rise with an increase in soiling and  
447 electricity prices. In addition, nonlinear degradation rate patterns can have an effect on the results of  
448 the NPV optimization algorithm, because they can influence the annual revenue rates.

449 The investigated site is characterized by a significant seasonal soiling profile, with a maximum power  
450 drop higher than 20% in summer, but an average energy loss lower than 3%. The results of the analysis  
451 can be considered valid for climatic conditions similar to the Mediterranean region. Despite that, the  
452 methodology presented in this work can be used to analyze soiling losses, identify the most  
453 advantageous cleaning schedule and calculate the profitability of PV systems in any location. The  
454 results of the sensitivity analysis are presented to show the variation of the trends depending on the  
455 value of the input parameters: degradation, inflation rate, electricity price and cleaning cost. For this  
456 reason, the benefits of a yearly optimized schedule should be considered on a case-by-case basis.  
457 More investigations should be conducted in future to characterize the correlation between the  
458 cleaning strategies and degradation rate for a larger number of sites that exhibit different soiling

459 profiles. Future work will also include the impact of non-uniform soiling and degradation rates that  
460 may occur across different inverters and strings within the same site.

## 461 Acknowledgements

462 The authors acknowledge Sonnedix for sharing commercial PV performance data. In particular, they  
463 wish to thank Juan M. Fernández and Ruth Prieto for the support in accessing and analyzing the data.

464 Leonardo Micheli's work was funded through the European Union's Horizon 2020 research and  
465 innovation programme under the NoSoilPV project (Marie Skłodowska-Curie grant agreement No.  
466 793120).

467 The work of Marios Theristis and Joshua S. Stein was supported by the U.S. Department of Energy's  
468 Office of Energy Efficiency and Renewable Energy (EERE) under the Solar Energy Technologies Office  
469 Award Number 34366. Sandia National Laboratories is a multimission laboratory managed and  
470 operated by National Technology & Engineering Solutions of Sandia, LLC, a wholly owned subsidiary  
471 of Honeywell International Inc., for the U.S. Department of Energy's National Nuclear Security  
472 Administration under contract DE-NA0003525. This paper describes objective technical results and  
473 analysis. Any subjective views or opinions that might be expressed in the paper do not necessarily  
474 represent the views of the U.S. Department of Energy or the United States Government.

475 The work of Florencia Almonacid and Eduardo F. Fernández was funded through the project ROM-PV  
476 which is supported under the umbrella of SOLAR-ERA.NET Cofund by the General Secretariat for  
477 Research and Technology (GSRT), the Ministry of Economy, Industry and Competitiveness – State  
478 Research Agency (MINECO-AEI) (ROM-PV, PCI2019-111852-2) and the Research and Innovation  
479 Foundation (RIF) of Cyprus. SOLAR-ERA.NET is supported by the European Commission within the EU  
480 Framework Programme for Research and Innovation HORIZON 2020 (Cofund ERA-NET Action, N°  
481 691664).

## 482 References

- 483 [1] B. Paudyal, M. Bolen, D. Fregosi, PV Plant Performance Loss Rate Assessment: Significance of  
484 Data Filtering and Aggregation, *Conf. Rec. IEEE Photovolt. Spec. Conf.* (2019) 866–869.  
485 <https://doi.org/10.1109/PVSC40753.2019.8981247>.
- 486 [2] A. Phinikarides, N. Kindyni, G. Makrides, G.E. Georghiou, Review of photovoltaic degradation  
487 rate methodologies, *Renew. Sustain. Energy Rev.* 40 (2014) 143–152.  
488 <https://doi.org/10.1016/j.rser.2014.07.155>.
- 489 [3] S. Lindig, I. Kaaya, K.A. Weis, D. Moser, M. Topic, Review of statistical and analytical  
490 degradation models for photovoltaic modules and systems as well as related improvements,  
491 *IEEE J. Photovoltaics.* 8 (2018) 1773–1786. <https://doi.org/10.1109/JPHOTOV.2018.2870532>.
- 492 [4] D.C. Jordan, T.J. Silverman, B. Sekulic, S.R. Kurtz, PV degradation curves: non-linearities and  
493 failure modes, *Prog. Photovoltaics Res. Appl.* 25 (2017) 583–591.  
494 <https://doi.org/10.1002/pip.2835>.
- 495 [5] M. Theristis, A. Livera, C.B. Jones, G. Makrides, G.E. Georghiou, J. Stein, Nonlinear photovoltaic  
496 degradation rates: Modeling and comparison against conventional methods, *IEEE J.*  
497 *Photovoltaics.* (2020).
- 498 [6] M. Theristis, A. Livera, L. Micheli, B. Jones, G. Makrides, G.E. Georghiou, J. Stein, Modeling  
499 nonlinear photovoltaic degradation rates, in: *IEEE 47th Photovolt. Spec. Conf.*, 2020.
- 500 [7] F.A. Mejia, J. Kleissl, Soiling losses for solar photovoltaic systems in California, *Sol. Energy.* 95  
501 (2013) 357–363. <https://doi.org/10.1016/j.solener.2013.06.028>.

502 [8] R. Conceição, I. Vázquez, L. Fialho, D. García, Soiling and rainfall effect on PV technology in rural  
503 Southern Europe, *Renew. Energy.* 156 (2020) 743–747.  
504 <https://doi.org/10.1016/j.renene.2020.04.119>.

505 [9] K. Ilse, L. Micheli, B.W. Figgis, K. Lange, D. Daßler, H. Hanifi, F. Wolfertstetter, V. Naumann, C.  
506 Hagendorf, R. Gottschalg, J. Bagdahn, Techno-Economic Assessment of Soiling Losses and  
507 Mitigation Strategies for Solar Power Generation, *Joule.* 3 (2019) 2303–2321.  
508 <https://doi.org/10.1016/j.joule.2019.08.019>.

509 [10] A. Massi Pavan, A. Mellit, D. De Pieri, The effect of soiling on energy production for large-scale  
510 photovoltaic plants, *Sol. Energy.* 85 (2011) 1128–1136.  
511 <https://doi.org/10.1016/j.solener.2011.03.006>.

512 [11] R. Conceição, H.G. Silva, L. Fialho, F.M. Lopes, M. Collares-Pereira, PV system design with the  
513 effect of soiling on the optimum tilt angle, *Renew. Energy.* 133 (2019) 787–796.  
514 <https://doi.org/10.1016/j.renene.2018.10.080>.

515 [12] M. Mani, R. Pillai, Impact of dust on solar photovoltaic (PV) performance: Research status,  
516 challenges and recommendations, *Renew. Sustain. Energy Rev.* 14 (2010) 3124–3131.  
517 <https://doi.org/10.1016/j.rser.2010.07.065>.

518 [13] National Renewable Energy Laboratory (NREL), Best Practices for Operation and Maintenance  
519 of Photovoltaic and Energy Storage Systems ; 3rd Edition., (2018) 153.  
520 <https://www.nrel.gov/research/publications.html>.

521 [14] A. Ullah, A. Amin, T. Haider, M. Saleem, N.Z. Butt, Investigation of soiling effects, dust chemistry  
522 and optimum cleaning schedule for PV modules in Lahore, Pakistan, *Renew. Energy.* 150 (2020)  
523 456–468. <https://doi.org/10.1016/j.renene.2019.12.090>.

524 [15] P. Besson, C. Munoz, G. Ramirez-Sagner, M. Salgado, R. Escobar, W. Platzer, Long-Term Soiling  
525 Analysis for Three Photovoltaic Technologies in Santiago Region, *IEEE J. Photovoltaics.* 7 (2017)  
526 1755–1760. <https://doi.org/10.1109/JPHOTOV.2017.2751752>.

527 [16] R.K. Jones, A. Baras, A. Al Saeeri, A. Al Qahtani, A.O. Al Amoudi, Y. Al Shaya, M. Alodan, S.A. Al-  
528 Hsaien, Optimized Cleaning Cost and Schedule Based on Observed Soiling Conditions for  
529 Photovoltaic Plants in Central Saudi Arabia, *IEEE J. Photovoltaics.* 6 (2016) 730–738.  
530 <https://doi.org/10.1109/JPHOTOV.2016.2535308>.

531 [17] S. You, Y.J. Lim, Y. Dai, C.H. Wang, On the temporal modelling of solar photovoltaic soiling:  
532 Energy and economic impacts in seven cities, *Appl. Energy.* 228 (2018) 1136–1146.  
533 <https://doi.org/10.1016/j.apenergy.2018.07.020>.

534 [18] P.M. Rodrigo, S. Gutierrez, L. Micheli, E.F. Fernández, F. Almonacid, Optimum cleaning schedule  
535 of photovoltaic systems based on levelised cost of energy and case study in central Mexico,  
536 *Sol. Energy.* 209 (2020) 11–20. <https://doi.org/10.1016/j.solener.2020.08.074>.

537 [19] E. Urrejola, J. Antonanzas, P. Ayala, M. Salgado, G. Ramírez-Sagner, C. Cortés, A. Pino, R.  
538 Escobar, Effect of soiling and sunlight exposure on the performance ratio of photovoltaic  
539 technologies in Santiago, Chile, *Energy Convers. Manag.* 114 (2016) 338–347.  
540 <https://doi.org/10.1016/j.enconman.2016.02.016>.

541 [20] M. Ciucci, Internal energy market, Fact Sheets Eur. Union. (2020).  
542 <https://www.europarl.europa.eu/factsheets/en/sheet/45/internal-energy-market> (accessed  
543 July 3, 2020).

544 [21] D.L. Alvarez, A.S. Al-Sumaiti, S.R. Rivera, Estimation of an Optimal PV Panel Cleaning Strategy  
545 Based on Both Annual Radiation Profile and Module Degradation, *IEEE Access.* 8 (2020) 63832–  
546 63839. <https://doi.org/10.1109/ACCESS.2020.2983322>.

547 [22] J.S. Stein, C. Robinson, B. King, C. Deline, S. Rummel, B. Sekulic, PV Lifetime Project: Measuring  
548 PV Module PerformanceDegradation: 2018 Indoor Flash TestingResults, 2018 IEEE 7th World  
549 Conf. Photovolt. Energy Conversion, WCPEC 2018 - A Jt. Conf. 45th IEEE PVSC, 28th PVSEC 34th

550 EU PVSEC. (2018) 771–777. <https://doi.org/10.1109/PVSC.2018.8547397>.

551 [23] L. Micheli, E.F. Fernández, J. Aguilera, F. Almonacid, Economics of seasonal photovoltaic soiling  
552 and cleaning optimization scenarios, *Energy*. In Press (n.d.).

553 [24] Global Modeling and Assimilation Office (GMAO), MERRA-2 tavg1\_2d\_slv\_Nx: 2d,1-  
554 Hourly,Time-Averaged,Single-Level,Assimilation,Single-Level Diagnostics V5.12.4, (2015).  
555 <https://doi.org/10.5067/VJAFPLI1CSIV>.

556 [25] W.F. Holmgren, C.W. Hansen, M.A. Mikofski, *pvlib python: a python package for modeling solar*  
557 *energy systems*, *J. Open Source Softw.* 3 (2018).  
558 <https://doi.org/https://doi.org/10.21105/joss.00884>.

559 [26] A.F. Souka, H.H. Safwat, Determination of the optimum orientations for the double-exposure,  
560 flat-plate collector and its reflectors, *Sol. Energy.* 10 (1966) 170–174.  
561 [https://doi.org/10.1016/0038-092X\(66\)90004-1](https://doi.org/10.1016/0038-092X(66)90004-1).

562 [27] ASHRAE standard 93-77, (n.d.).

563 [28] D.L. King, W.E. Boyson, J.A. Kratochvill, Photovoltaic array performance model, Albuquerque,  
564 New Mexico, 2004. <https://doi.org/10.2172/919131>.

565 [29] F. Kasten, A.T. Young, Revised optical air mass tables and approximation formula, *Appl. Opt.* 28  
566 (1989) 4735–4738. <https://doi.org/10.1364/AO.28.004735>.

567 [30] C. Gueymard, Critical analysis and performance assessment of clear sky solar irradiance models  
568 using theoretical and measured data, *Sol. Energy.* 51 (1993) 121–138.  
569 [https://doi.org/10.1016/0038-092X\(93\)90074-X](https://doi.org/10.1016/0038-092X(93)90074-X).

570 [31] I. Reda, A. Andreas, Solar position algorithm for solar radiation applications, *Sol. Energy.* 76  
571 (2004) 577–589. <https://doi.org/10.1016/j.solener.2003.12.003>.

572 [32] International Electrotechnical Commission, Photovoltaic system performance – Part 1:  
573 Monitoring (IEC 61724-1, Edition 1.0, 2017-03), (2017).

574 [33] M.G. Deceglie, L. Micheli, M. Muller, Quantifying Soiling Loss Directly From PV Yield, *IEEE J.*  
575 *Photovoltaics.* 8 (2018) 547–551. <https://doi.org/10.1109/JPHOTOV.2017.2784682>.

576 [34] L. Micheli, M. Muller, An investigation of the key parameters for predicting PV soiling losses,  
577 *Prog. Photovoltaics Res. Appl.* 25 (2017) 291–307. <https://doi.org/10.1002/pip.2860>.

578 [35] L. Micheli, M.G. Deceglie, M. Muller, Predicting photovoltaic soiling losses using environmental  
579 parameters: An update, *Prog. Photovoltaics Res. Appl.* 27 (2019) 210–219.  
580 <https://doi.org/10.1002/pip.3079>.

581 [36] L. Micheli, M. Muller, E.F. Fernández, F.M. Almonacid, Change Point Detection: An Opportunity  
582 to Improve PV Soiling Extraction, in: *IEEE 45th Photovolt. Spec. Conf.*, 2020.

583 [37] A. Kimber, L. Mitchell, S. Nogradi, H. Wenger, The Effect of Soiling on Large Grid-Connected  
584 Photovoltaic Systems in California and the Southwest Region of the United States, in: *Photovolt. Energy Conversion, Conf. Rec. 2006 IEEE 4th World Conf.*, 2006: pp. 2391–2395.

585 [38] B. Figgis, A. Ennaoui, S. Ahzi, Y. Rémond, Review of PV soiling particle mechanics in desert  
586 environments, *Renew. Sustain. Energy Rev.* 76 (2017) 872–881.  
587 <https://doi.org/10.1016/j.rser.2017.03.100>.

588 [39] K.K. Ilse, B.W. Figgis, V. Naumann, C. Hagendorf, J. Bagdahn, Fundamentals of soiling processes  
589 on photovoltaic modules, *Renew. Sustain. Energy Rev.* 98 (2018) 239–254.  
590 <https://doi.org/10.1016/j.rser.2018.09.015>.

591 [40] L. Micheli, E.F. Fernandez, M. Muller, F. Almonacid, Extracting and Generating PV Soiling  
592 Profiles for Analysis, Forecasting, and Cleaning Optimization, *IEEE J. Photovoltaics.* 10 (2020)  
593 197–205. <https://doi.org/10.1109/JPHOTOV.2019.2943706>.

594 [41] J. Zorrilla-Casanova, M. Piliougine, J. Carretero, P. Bernaola-Galván, P. Carpena, L. Mora-López,  
595 M. Sidrach-de-Cardona, Losses produced by soiling in the incoming radiation to photovoltaic

597 modules, *Prog. Photovoltaics Res. Appl.* 20 (2012) n/a-n/a. <https://doi.org/10.1002/pip.1258>.

598 [42] R. Appels, B. Lefevre, B. Herteleer, H. Goverde, A. Beerten, R. Paesen, K. De Medts, J. Driesen,  
599 J. Poortmans, Effect of soiling on photovoltaic modules, *Sol. Energy.* 96 (2013) 283–291.  
600 <https://doi.org/10.1016/j.solener.2013.07.017>.

601 [43] National Renewable Energy Laboratory, Photovoltaic modules soiling map, (2018).  
602 <https://www.nrel.gov/pv/soiling.html> (accessed May 18, 2018).

603 [44] F. Kersten, P. Engelhart, H.C. Ploigt, A. Stekolnikov, T. Lindner, F. Stenzel, M. Bartzsch, A. Szpeth,  
604 K. Petter, J. Heitmann, J.W. Muller, A new mc-Si degradation effect called LeTID, 2015 IEEE  
605 42nd Photovolt. Spec. Conf. PVSC 2015. (2015). <https://doi.org/10.1109/PVSC.2015.7355684>.

606 [45] M. Theristis, V. Venizelou, G. Makrides, G.E. Georghiou, Energy yield in photovoltaic systems,  
607 in: *McEvoy's Handb. Photovoltaics Fundam. Appl.*, 2018: pp. 671–713.  
608 <https://doi.org/10.1016/B978-0-12-809921-6.00017-3>.

609 [46] D.L. Staebler, C.R. Wronski, Reversible conductivity changes in discharge-produced amorphous  
610 Si, *Appl. Phys. Lett.* 31 (1977) 292–294. <https://doi.org/10.1063/1.89674>.

611 [47] M.G. Deceglie, T.J. Silverman, S.W. Johnston, J.A. Rand, M.J. Reed, R. Flottemesch, I.L. Repins,  
612 Light and Elevated Temperature Induced Degradation (LeTID) in a Utility-Scale Photovoltaic  
613 System, *IEEE J. Photovoltaics* 10 (2020) 1084–1092.  
614 <https://doi.org/10.1109/JPHOTOV.2020.2989168>.

615 [48] D.L. Talavera, E. Muñoz-Cerón, J.P. Ferrer-Rodríguez, P.J. Pérez-Higueras, Assessment of cost-  
616 competitiveness and profitability of fixed and tracking photovoltaic systems: The case of five  
617 specific sites, *Renew. Energy.* 134 (2019) 902–913.  
618 <https://doi.org/10.1016/j.renene.2018.11.091>.

619 [49] G. Jiménez-Castillo, F.J. Muñoz-Rodriguez, C. Rus-Casas, D.L. Talavera, A new approach based  
620 on economic profitability to sizing the photovoltaic generator in self-consumption systems  
621 without storage, *Renew. Energy.* 148 (2020) 1017–1033.  
622 <https://doi.org/10.1016/j.renene.2019.10.086>.

623 [50] C. Himmelskamp, Fotovoltaica en España: breve resumen de tarifas, del desarrollo de  
624 proyectos y la financiación de instalaciones fotovoltaicas, *Pv-Magazine.* (2019).  
625 <https://www.pv-magazine.es/2019/03/08/fotovoltaica-en-espana-breve-resumen-de-tarifas-del-desarrollo-de-proyectos-y-la-financiacion-de-instalaciones-fotovoltaicas/> (accessed July 6,  
626 2020).

627 [51] OMIE, Informes anuales, (2020). <https://www.omie.es/es/publicaciones/informe-anual>  
628 (accessed May 18, 2020).

629 [52] Eurostat. European Commission, Energy statistics - prices of natural gas and electricity, (2020).  
630 <http://ec.europa.eu/eurostat/web/energy/data/database> (accessed May 17, 2020).

631 [53] S. Enkhhardt, Europe has now 8.4 GW of planned and built PV projects under PPAs, *Pv-Magazine.*  
632 (2020). <https://www.pv-magazine.com/2020/01/29/europe-has-now-8-4-gw-of-planned-and-built-pv-projects-under-ppas/> (accessed July 6, 2020).

633 [54] IEA PVPS, Trends in photovoltaic applications 2019, 2020. <https://iea-pvps.org/wp-content/uploads/2020/02/5319-iea-pvps-report-2019-08-1r.pdf>.

634 [55] The World Bank, Inflation, consumer prices (annual %), (2020).  
635 <https://data.worldbank.org/indicator/FP.CPI.TOTL.ZG> (accessed May 18, 2020).

636

637

638

639